

1 **Title: Indoxyl sulfate (IS)-mediated immune dysfunction provokes endothelial damage**  
2 **in patients with end-stage renal disease (ESRD)**

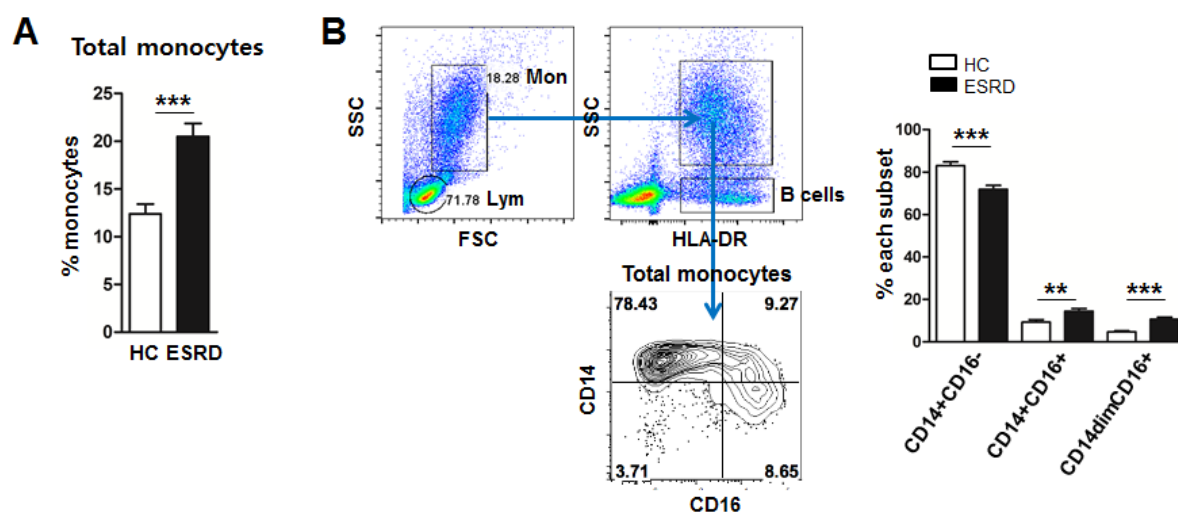
3  
4 **Authors:** Hee Young Kim, Tae-Hyun Yoo, Yuri Hwang, Ga Hye Lee, Bonah Kim, Ji yeon  
5 Jang, Hee Tae Yu, Min Chang Kim, Joo-Youn Cho, Chan Joo Lee, Hyeon Chang Kim,  
6 Sungha Park and Won-Woo Lee

7  
8  
9  
10 **Supplementary Material and Methods**

11 **Measurement of ROS**

12 Cells were incubated with 10  $\mu$ M 5-(and-6)-chloromethyl-2',7'-dichlorodihydrofluorescein  
13 diacetate, acetyl ester (CM-H<sub>2</sub>DCFDA; Invitrogen, Carlsbad, CA) for 30 min, followed by washing  
14 with DPBS, and were treated for the indicated times with IS in the presence of NAC (N-acetyl-  
15 cysteine; Sigma-Aldrich, St. Louis, MO), ROS inhibitor or GNF351 (Calbiochem, San Diego, CA),  
16 AhR antagonist. ROS production by the cells was analyzed using flow cytometry.

19 **Supplementary figures**



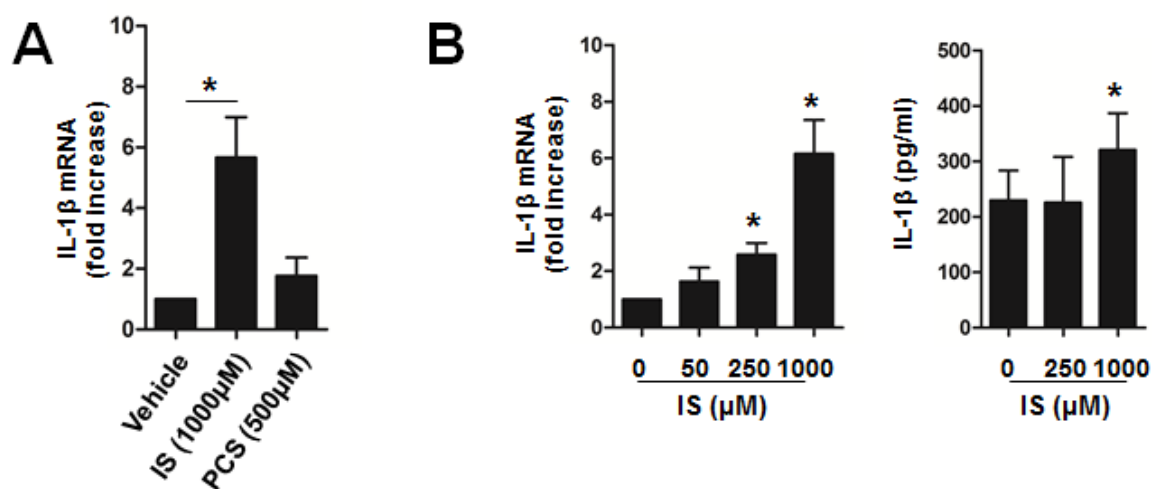
20

21 **Supplementary figure 1. CD16<sup>+</sup> monocytes are significantly expanded in ESRD patient.**

22 (A) Frequencies (%) of total monocytes (defined as HLA-DR<sup>+</sup>CD14<sup>dim/+</sup>) among PBMCs were  
 23 analyzed in ESRD patients (n=50) and age-matched HCs (n=28). Monocytes were defined as cells  
 24 expressing HLA-DR, but not lineage markers, such as CD3 (T cells), CD19 (B cells), or CD56 (NK  
 25 cells) by flow cytometry. (B) Frequencies (%) of three distinct monocyte subsets were compared  
 26 between ESRD patients and HCs. Total monocytes were further subdivided into three subsets by their  
 27 expression of CD14 and CD16. Representative contour plot of peripheral monocytes from an ESRD  
 28 patient. Bar graphs show the mean ± SEM. \*\* = *p*<0.01, and \*\*\* = *p*<0.001 by two-tailed unpaired *t*-  
 29 test.

30

31



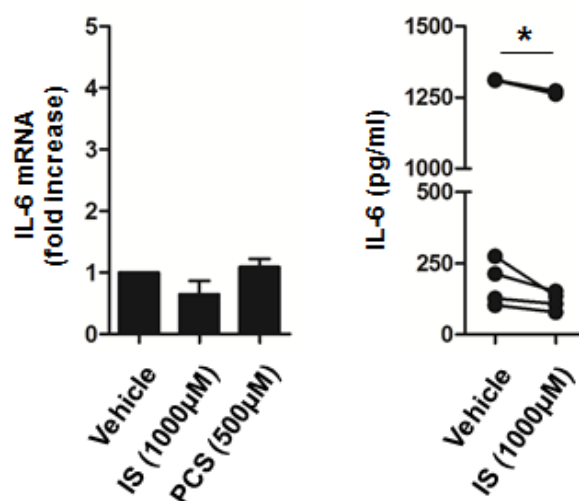
32

33

34 **Supplementary figure 2. Indoxyl sulfate (IS) is responsible for enhanced IL-1 $\beta$  expression by**  
35 **human monocytes.**

36 (A) Purified monocytes were stimulated with 1,000  $\mu$ M of IS or 500  $\mu$ M of PCS for 24 hr and then  
37 IL-1 $\beta$  mRNA expression was analyzed by real-time RT-PCR. (B) Purified monocytes were stimulated  
38 with IS at the indicated concentrations. The expression of IL-1 $\beta$  mRNA was analyzed by real-time  
39 RT-PCR after a 24 hr stimulation (**left**) and its protein level was quantified by ELISA at 48 hr post-  
40 stimulation (**right**). Expression of  $\beta$ -actin was used as a normalization control for real-time RT-PCR  
41 analysis. Bar graphs show the mean  $\pm$  SEM of three (A) and five to seven (B). \* =  $p < 0.05$  by two-  
42 tailed paired  $t$ -test (A and B).

43



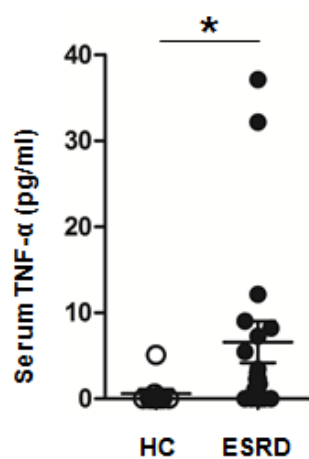
44

45 **Supplementary figure 3. No induction of IL-6 is observed in monocytes treated with both IS and**  
46 **PCS.**

47

48 **(Left)** Purified monocytes were stimulated with 1,000 µM of IS or 500 µM of PCS for 24 hr and then  
49 IL-6 mRNA expression was analyzed by real-time RT-PCR. **(Right)** Purified monocytes were  
50 stimulated with 1,000 µM of IS. The amount of IL-6 in the culture supernatant was quantified by  
51 ELISA at 48 hr post-stimulation. Expression of β-actin was used as a normalization control for real-  
52 time RT-PCR analysis. Bar graphs show the mean ± SEM of three **(Left)** and six **(Right)**. \* =  $p < 0.05$   
53 by two-tailed paired *t*-test.

54



55

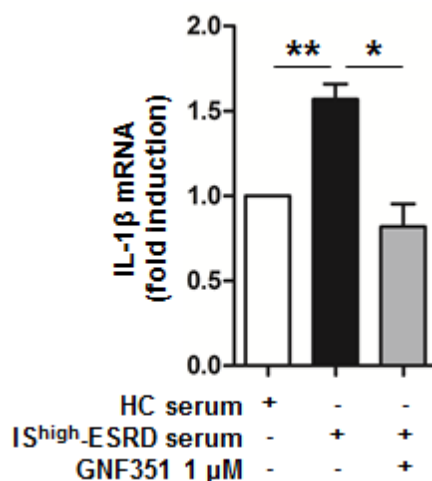
56 **Supplementary figure 4. Serum TNF- $\alpha$  level is higher in ESRD patients than in healthy controls.**

57

58 The amount of TNF- $\alpha$  in serum was quantified by ELISA and compared between ESRD patients  
59 (n=19) and age-matched HCs (n=10). \* =  $p < 0.05$  by two-tailed unpaired  $t$ -test.

60

61



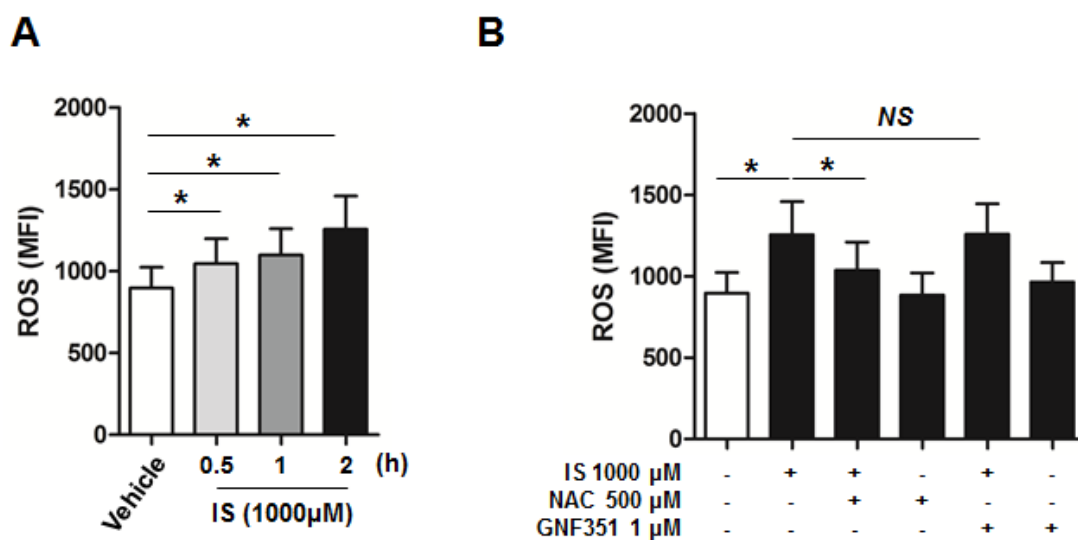
62

63 **Supplementary figure 5. Uremic sera-activated induction of IL-1 $\beta$  is abrogated in monocytes by**  
64 **GNF351, AhR antagonists.**

65

66 Sera were pooled from patients with the top 10 (IS<sup>higher</sup>-ESRD) IS serum concentrations. As a control,  
67 sera from healthy controls were pooled. Monocytes isolated from healthy controls were treated with  
68 30% (v/v) of the indicated sera for 24 hr with or without 1  $\mu$ M of GNF351, AhR antagonists. Gene  
69 expression levels were analyzed by real-time RT-PCR. Expression of  $\beta$ -actin was used as a  
70 normalization control. Bar graphs show the mean  $\pm$  SEM of four to six independent experiments. \* =  
71  $p < 0.05$  and \*\* =  $p < 0.01$  by two-tailed paired  $t$ -test.

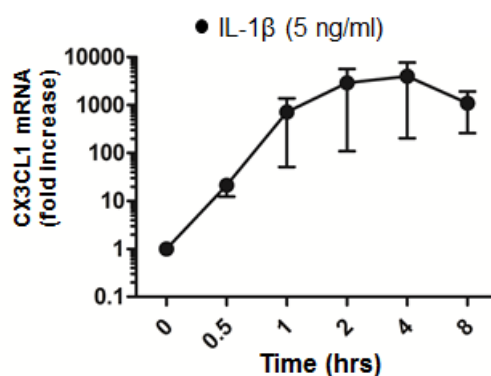
72



73

74 **Supplementary figure 6.** Purified monocytes were incubated with 10 μM 5-(and-6)-chloromethyl-  
 75 2',7'-dichlorodihydrofluorescein diacetate, acetyl ester (CM-H<sub>2</sub>DCFDA, Invitrogen) for 30 min and  
 76 were washed with DPBS. The monocytes were treated for 2 hr with IS in the presence of NAC (N-  
 77 acetyl-cysteine), ROS inhibitor or GNF351, AhR antagonists. The level of ROS production was  
 78 analyzed using flow cytometry. Bar graphs show the mean ± SEM of four independent experiments (**A**  
 79 and **B**). \* =  $p < 0.05$  by two-tailed paired *t*-test. NS indicates not significant.

80



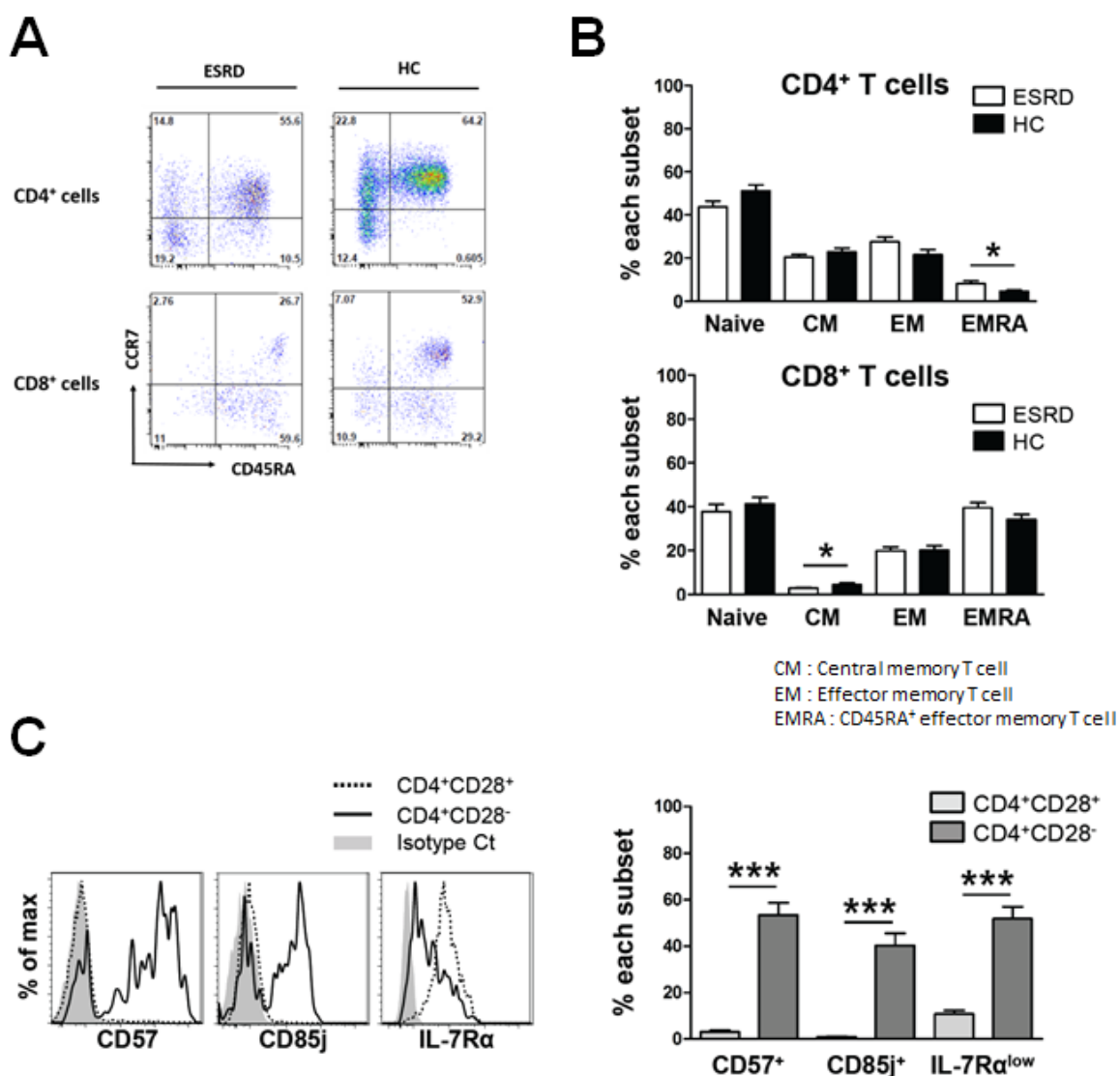
81

82 **Supplementary figure 7. IL-1 $\beta$  markedly upregulates CX3CL1 production by HUVECs**

83 HUVECs were stimulated with IL-1 $\beta$  (5 ng/ml) for up to 8 hours and CX3CL1 mRNA expression was  
84 analyzed by real-time RT-PCR at the indicated time-points. Expression of  $\beta$ -actin was used as a  
85 normalization control. Bar graphs show the mean  $\pm$  SEM of three independent experiments.

86





87

88 **Supplementary figure 8. Phenotypic characterization of T cells in patients with ESRD**

89 Phenotypic characterization of peripheral T cells in peripheral blood mononuclear cells (PBMCs) of  
 90 ESRD patients (n=50) and age-matched HCs (n=28) by flow cytometry. **(A)** Distribution of functional  
 91 T-cell subsets defined by the expression pattern of CD45RA and CCR7 in CD4<sup>+</sup> and CD8<sup>+</sup> T cells.  
 92 Naive (CD45RA<sup>+</sup>CCR7<sup>+</sup>), central memory (CM: CD45RA<sup>+</sup>CCR7<sup>+</sup>), effector memory (EM: CD45RA<sup>+</sup>  
 93 CCR7<sup>-</sup>), and CD45RA<sup>+</sup> effector memory (EMRA: CD45RA<sup>+</sup>CCR7<sup>-</sup>). **(B)** Frequencies (%) of CD28<sup>-</sup>  
 94 cells in CD4<sup>+</sup> and CD8<sup>+</sup> T cells. **(C)** Representative flow cytometric analysis of senescence marker  
 95 (CD57, CD85j, and IL-7R $\alpha$ ) expression on CD4<sup>+</sup>CD28<sup>+</sup> and CD4<sup>+</sup>CD28<sup>-</sup> T cells. **(D)** Frequency (%)  
 96 of CD57<sup>+</sup>, CD85j<sup>+</sup>, and IL-7R $\alpha$ <sup>low</sup> cells in CD4<sup>+</sup>CD28<sup>+</sup> and CD4<sup>+</sup>CD28<sup>-</sup> T cell populations (n=24 or  
 97 32) of ESRD patients. Bars graphs show the mean  $\pm$  SEM. \* =  $p < 0.05$ , \*\* =  $p < 0.01$ , and \*\*\* =  
 98  $p < 0.001$  by two-tailed unpaired **(A and B)** or paired *t*-test **(C)**.  
 99